

Reply to reviewers

September 12, 2019

We would like to thank the two reviewers for their feedback and suggestions to improve the article. In the proceeding sections, the reviewers comments are copied and answered per comment (blue color). An additional document is provided that highlights all modifications with respect to the initial submitted version.

Reviewer 1

The manuscript presents a velocity-independent actuator disk method to reduce computational costs for numerical simulations of wind farm flows. The annual energy production (AEP) of a rectangular 5*5 wind farm consisting of NREL-5MW turbines is computed including different wind speeds and directions. The results show that using the new method can reduce computational costs by a factor 2-3. It is indeed useful to develop RANS simulations with lower computational costs, and I appreciate the authors' efforts to address this issue. However, I have some concerns regarding the methodology suggested in this paper. My main concern is associated with validity of the concept of a velocity-independent actuator disk. Any change in the incoming velocity can affect wind flow distribution in different ways. In a turbulent boundary layer, any change in the incoming velocity at hub height affects the mean flow shear and size of large turbulent eddies, among other effects. The proposed technique is likely to capture effects of wind speed change on the thrust force. However, it seems that it does not account for changes in flow physics caused by a change in the incoming wind speed.

We do not share this concern because the inflow turbulence length scale ℓ in our RANS setup follows the neutral atmospheric surface layer: $\ell = \kappa z$, with κ as the Von Karman constant and z as the height. This turbulence length scale is independent of the wind speed. The turbulence length scale in wind turbine wake deviates from the inflow turbulence length scale, but the velocity deficit normalized by a inflow wind speed, is not dependent on the inflow wind speed. We understand from the review process that this concept might not be well know. Therefore, we have now added an Appendix showing a proof of the Reynolds number independence of the RANS simulations of a single wind turbine wake in a neutral atmospheric surface layer, for a wind speed at hub height of 1, 10 and 100 m/s, for two thrust coefficients and two turbulence intensities. These wind speeds correspond to the following Reynolds numbers based on the rotor diameter: 8.7×10^6 , 8.7×10^7 and 8.7×10^8 (where the kinematic molecular viscosity is set to $1.46 \times 10^{-5} \text{ m}^2 \text{ s}^{-1}$).

Other more specific comments can be found below:

1. Page 1, line 20: Apart from the turbulence intensity, the integral length scale is also an important factor as it represents the size of largest turbulent structures in the flow.

See previous answer.

2. Figure 1: Please clarify how the curve shown for a different scaling factor "s" is computed.

We use the scaling factor s from equation 1, to multiply $\langle U_{AD} \rangle$ in the $C_t-\langle U_{AD} \rangle$ relation. Figure 1 shows this for $s = 1.2$. We have added the following in Section 2.2: "We multiply $\langle U_{AD} \rangle$ in the $C_T^*-\langle U_{AD} \rangle$ by s ."

3. Page 3, line 6: How many simulations are performed to estimate $C_t^*-\langle U_{AD} \rangle$? Please provide more information about this.

We have added: "Prior to the wind farm simulations, a $C_T^*-\langle U_{AD} \rangle$ relation is calculated from a RANS-AD simulation of one AD for each wind speed between 4 and 25 m/s, for every 1 m/s, using the known

C_T curve. We only use one RANS-AD simulation with a constant global inflow, where C_T is updated every time the simulation for a previous C_T has converged.”

4. Page 5, line 32: The convergence error is used in this study as the AEP computed by the base case is already available. Please elaborate how this criterion can be used if one aims at using the new technique without a prior knowledge on the true value of AEP.

The convergence error in the AEP was calculated using several AEP calculations with different levels of convergence criteria. In this work, we have only looked at one wind farm layout, one wind turbine type and one level of turbulence intensity. The change of one of these may lead to the need for stricter convergence criterium. We normally set a quite conservative level of convergence. One could investigate how changes in wind farm layout, wind turbine type and turbulence intensity affect the convergence criterium, but this is out of the scope of the present work. We have discussed the level of convergence in Section 5 because it has a high impact on the computational cost. If one is interested in a rough estimate of the AEP, a less strict convergence criterium could be considered to get a quick result.

5. Minor editorial comments:

- (a) Page 1, line 13: I think “relative” should be replaced by “relatively”.
- (b) Page 1, line 14: “be” is missed in “that can used”.
- (c) Page 2, line 5: “is” should be removed in “This is strategy ...”
- (d) Page 5, line 5: “This an optimization ... ” is grammatically incorrect.

We have corrected these four typos.

Reviewer 2

This brief communication describes the extension of a methodology for calculating the AEP of wind farms. The extension leads to an acceleration of the calculation compared to the baseline method. The description of the basic method along with the introduced simplifications and assumptions can only be comprehended if one is familiar with the corresponding detailed publications referenced by the authors. This is fine for a brief communication. But I suggest that the authors refer to corresponding published works every time when assumptions or simplifications are explicitly mentioned (see also below).

If I understood the manuscript correctly, the novelty of the method concern a scaling of the thrust coefficient C_T to mimic the influence of changes in wind speed instead of actually changing the wind speed in the CFD calculations. This leaves the global flow field unchanged and the modified thrust coefficient results in more local changes of the wind field in the area of the turbines and their wakes. By this and by a clever sequence of restarts based on converged previous calculations, the authors were able to reduce the computation time by a factor of 2-3.

Methods for fast, CFD-based AEP calculation of wind farms are important and work on acceleration of the calculation process are relevant. Therefore, I basically support the publication of this brief communication. However, the description of the method and the new aspects is very difficult for the reader to understand, especially if he does not know the publications of the baseline method. The authors should therefore revise the text taking into account the comments below, describe page 3 in some more detail and include citations at all points where assumptions and simplifications are mentioned.

Specific comments and remarks:

1. Abstract: The last two sentences of the abstract contain important assumptions of the new aspects of the method and should be picked up at page 3 where the velocity scaling is introduced.
We have extended the description of the new AD control method in Section 2.2.
2. Introduction: In atmospheric flow properties like integral length scale, turbulence intensity, shear profile etc. depend on wind speed. It is unclear whether these properties are also scaled in the proposed method or if the impact of wind speed is neglected. This should be mentioned and justified.
Reviewer 1 had a very similar comment about this. Please find the answer in the reply to Reviewer 1.

3. 2.2, 1.2-3 p.3: Unless the reader already knows the cited previous work, it is unclear that the average of the square velocity is used to obtain the scaled thrust coefficient c_T^* . Please add shortly this information.

We added how C_T^* is calculated: "..., which can be calculated as $C_T^* = (U_H/\langle U_{AD} \rangle)^2$, with U_H as the freestream wind speed at hub height." In addition, we have also added how C_P^* is calculated.

4. 2.2: 1. 4-5 p.3: "The thrust force distribution of the AD is based on a normalized thrust force distribution". For the NREL 5 MW wind turbine, the thrust force distribution almost linearly scales with the rotor thrust coefficient c_T only below rated conditions and is flattened at higher wind speeds. Please add some information about how the thrust distribution is scaled with your method and how you deal with above rated situations.

The AD method from van der Laan et al. (2015), assumes that the normalized force distribution does not change with wind speed, and this assumption is also made in the present work. The reviewer is right that the thrust force distribution is different above rated wind speeds and our assumption is violated. One could argue that the wake effects above rated are rather small due to the low thrust coefficient. Hence, the impact of our constant normalized thrust force distribution is expected to be small. In addition, Simisiroglou et al. (2017) has shown that the effect of different force distributions (for the same total thrust force) has only an impact on the near wake, while the far wake is very similar, especially when atmospheric turbulence is included. We have added this discussion to Section 2.2.

5. 2.2: 1. 6 p.3: Please define what is meant with "standard CT curve" and give some reference.

We have changed "standard" to "known" C_T curve to make this more clear.

6. 2.2, p.3: It is unclear to me how the scaling parameter s is used within the simulation. Please clarify and give some justification.

The scaling parameter s is used to multiply $\langle U_{AD} \rangle$ in the C_t - $\langle U_{AD} \rangle$ relation. Figure 1 shows this for $s = 1.2$. We have the following in Section 2.2: "We multiply $\langle U_{AD} \rangle$ in the C_T^* - $\langle U_{AD} \rangle$ by s ."

7. Conclusions: 1.11-12 p.6: The application of this method to complex terrain situations should first be proven. In complex terrains, flow inclination, changes of the wind direction over the rotor disc, flow separation and large scale turbulent structures are apparent. These effects do not necessarily linearly scale with the inflow velocity. I am looking forward to your results.

For RANS simulations of complex terrain using a logarithmic inflow, the speed up factor is independent of the wind speed due to the Reynolds number independence. Note that the viscous sub layer near the wall is not resolved since we use a rough wall boundary condition. We have added a reference discussing the Reynolds number independence: Troen et al. (2014) in Section 3. The reviewer could also have a look at a presentation given by Bechmann (2014), where the Reynolds number independence was shown by RANS simulations of the speed up factor over complex terrain.

The reviewer is right that we have not applied the new wind speed independent AD control method in the present work. Therefore, we have removed the statement about the application to complex terrain in the conclusion.

References

- A. Bechmann. How to use CFD for long-term energy assessments. Presentation at Wind Resource Assessment Conference, 2014. URL https://orbit.dtu.dk/files/117048848/ABechmann_How_to_use_CFD.pdf.
- N. Simisiroglou, S.-P. Breton, and S. Ivanell. Validation of the actuator disc approach using small-scale model wind turbines. *Wind Energy Science*, 2(2):587–601, 2017. doi: 10.5194/wes-2-587-2017. URL <https://www.wind-energ-sci.net/2/587/2017/>.
- I. Troen, A. Bechmann, M. C. Kelly, N. N. Sørensen, P.-E. Réthoré, D. Cavar, and H. E. Jørgensen. Complex terrain wind resource estimation with the wind-atlas method: Prediction errors using linearized and nonlinear CFD micro-scale models. In *Proceedings of European Wind Energy Association*, 2014. URL https://orbit.dtu.dk/files/112008174/Complex_terrain_wind_resource.pdf.

M. P. van der Laan, N. N. Sørensen, P.-E. Réthoré, J. Mann, M. C. Kelly, and N. Troldborg. The $k\text{-}\varepsilon\text{-}f_p$ model applied to double wind turbine wakes using different actuator disk force methods. *Wind Energy*, 18(12):2223–2240, December 2015. doi: 10.1002/we.1816.

Brief communication: Wind speed independent actuator disk control for faster AEP calculations of wind farms using CFD

Maarten Paul van der Laan¹, Søren Juhl Andersen², and Pierre-Elouan Réthoré¹

¹Technical University of Denmark, DTU Wind Energy, Risø Campus, Frederiksborgvej 399, 4000 Roskilde, Denmark

²Technical University of Denmark, DTU Wind Energy, Lyngby Campus, Anker Engelunds Vej 1, 2800 Lyngby, Denmark

Correspondence: Maarten Paul van der Laan (plaa@dtu.dk)

Abstract. A simple wind speed independent actuator disk control method is proposed that can be applied to speed up annual energy production calculations of wind farms using Reynolds-averaged Navier-Stokes simulations. The new control method allows the user to simulate the effect of different wind speeds in one simulation by scaling a calibrated thrust coefficient curve, while keeping the inflow constant. Since the global flow is not changed, only the local flow around the actuator disks needs be recalculated from a previous converged result, which reduces the number of required iterations and computational effort by a factor of about 2-3.

1 Introduction

Wind turbines wakes cause energy losses in wind farms (Barthelmie et al., 2007) and increase blade fatigue loads. The energy losses can be minimized by optimizing the wind farm layout and wind farm control. Fast engineering wake models (Göçmen et al., 2016) are often used to calculate wake effects in optimization routines; however, their accuracy is not guaranteed and higher fidelity wake models are required to validate the annual energy production (AEP) of an optimized wind farm layout. Assessing the AEP for a given wind farm requires in the order of 10^3 computations to account for all wind speeds and wind directions. Reynolds-averaged Navier-Stokes (RANS) is a [relative-relatively](#) fast, yet high-fidelity, computational fluid dynamics method that can [be](#) used for this purpose (van der Laan et al., 2015b), although it is still computationally expensive compared to the traditional engineering approaches.

The wind turbines in RANS are often represented by actuator disks (AD), where the wind turbine forces are implemented as a sink term in the momentum equations. The Reynolds number of the RANS-AD simulations, based on a rotor diameter of 100 m, is in the order of 10^7 - 10^8 for a wind speed range of 4-25 m s^{-1} . For these large Reynolds numbers, RANS simulations of a single AD are Reynolds number independent. In other words, the wake deficit, normalized by the inflow wind speed, does not depend on the inflow wind speed, but only depends on the thrust coefficient and atmospheric conditions as ambient turbulence intensity and atmospheric stratification. [A proof of the Reynolds number independence of our RANS simulations for a single AD is presented in Appendix A. The Reynolds number independence only holds if the inflow scales by a velocity scale, i.e. the friction velocity. This is true for atmospheric surface layer profiles following Monin-Obukhov Similarity Theory, where the turbulence length scale is also invariant of the wind speed.](#) For RANS-AD simulations of wind farms, the thrust coefficient

varies within the wind farm, which means that one still needs to simulate multiple wind speed cases despite the Reynolds number independence of the flow **problem**.

In previous work (van der Laan et al., 2015a), an AD control method was developed for RANS simulations of interacting ADs, where an alternative thrust coefficient C_T^* was used that is dependent on the local AD velocity, averaged over the AD: $\langle U_{AD} \rangle$. This avoids the necessity of a freestream wind speed (which is not trivial for an AD operating in a wake) to look up the thrust coefficient. The $C_T^*-\langle U_{AD} \rangle$ curve was calculated from single RANS-AD simulations. In the present work, the AD control method is made wind speed independent by a simple additional scaling of $\langle U_{AD} \rangle$, as explained in Sect. 2.2. This **is** strategy is related to the work of Andersen (2014), where non-dimensional large-eddy simulations of wind turbines represented by actuator lines were coupled to an aero-elastic model that uses a dimensional controller. The extended AD control method can be utilized to perform one RANS-AD simulation to simulate the effect of different wind speeds without changing the inflow, thereby reducing the computational effort of a full AEP calculation by a factor of about 2-3 compared to using different inflow wind speeds.

2 Methodology

2.1 Wind farm simulations

The RANS-AD methodology used for our wind farm simulations are described in previous work (van der Laan et al., 2015b), and a brief summary is presented here. The RANS equation are solved in EllipSys3D, the in-house finite volume flow solver of DTU Wind Energy, initially developed by Sørensen (1994); Michelsen (1992). The $k-\varepsilon-f_P$ turbulence model is employed (van der Laan et al., 2015c), which has been developed for RANS-AD simulations using a neutral atmospheric surface layer. The 3D flow domain represents a Cartesian domain with dimensions ($L_x = 850D$, $L_y = 830$ and $L_z = 10D$), for the streamwise (x), lateral (y) and vertical directions (z), respectively. In the center of flow domain, a uniformly spaced domain is defined with dimensions $54D \times 35D \times 3D$, in which the wind turbines wakes of 5×5 ADs are resolved. The ADs represent a wind farm of 25 NREL-5MW wind turbines (Jonkman et al., 2009) positioned in a rectangular layout with an inter spacing of 5 rotor diameters D . The uniformly spaced domain around the wind farm has a cell size equal to $D/8$, following a grid refinement study of previous work (van der Laan et al., 2015c). The cells sizes are grown while moving away from the wind farm. The grid consists of 352 blocks of 32^3 cells, which adds up 11.5 million cells. One CPU per block is used in the simulations (352 CPUs in total). The boundary at $x = 0$ and $z = L_z$ are inlet conditions, at which a logarithmic inflow profile for the streamwise velocity U , turbulent kinetic energy k and dissipation of the turbulent kinetic energy ε is set following Richards and Hoxey (1993). Periodic conditions are imposed on the lateral boundaries and an outflow boundary is set at $x = L_x$, at which all gradients in the streamwise direction are assumed to be zero. The ground is set as a rough wall boundary condition following Sørensen et al. (2007). An offshore ambient turbulence intensity (based on k) of 6 % is set at the wind turbine hub height of 90 m, by using a (uniform) roughness length of 1.9×10^{-4} m. The convergence criterion in the RANS-AD simulations is set strict enough to calculate the AEP within a 0.02 % convergence error.

2.2 Wind speed independent AD control

The new AD force control method is an extension of previous work (van der Laan et al., 2015a), where the total thrust on the AD is defined by $F_{\text{thrust}} = 1/2 C_T^* \rho A \langle U_{AD} \rangle^2$. Here, C_T^* is the thrust coefficient based on the local AD velocity, averaged over the AD $\langle U_{AD} \rangle$, which can be calculated as $C_T^* = (U_H / \langle U_{AD} \rangle)^2$, with U_H as the freestream wind speed at hub height. The thrust force distribution of the AD is based on a normalized thrust force distribution computed by a detached eddy simulation of a blade-resolved NREL-5MW rotor for a below-rated wind speed of 8 m s^{-1} (Réthoré et al., 2014). The normalized thrust force distribution is scaled by C_T^* and $\langle U_{AD} \rangle$. Hence, it is assumed that the thrust force distribution, based on a below-rated wind speed, does not change shape. This is generally not true for above-rated wind speeds, where the thrust force distribution is typically more uniform. However, Simisiroglou et al. (2017) has shown that the effect of different thrust force distributions (with constant total thrust force) on the velocity deficit is mainly visible in the near wake, while the far wake is almost unaffected, especially when atmospheric turbulence is present. In addition, the wake effects above-rated wind speeds are small due to the low thrust coefficient. Hence, the effect of our assumed thrust force distribution on the annual energy production is expected to be small.

Prior to the wind farm simulations, a $C_T^*-\langle U_{AD} \rangle$ relation is calculated from a RANS-AD simulation of one AD for each wind speed using the standard between 4 and 25 m/s, for every 1 m/s, using the known C_T curve. We only use one RANS-AD simulation with a constant global inflow, where C_T is updated every time the simulation for a previous C_T has converged. The $C_T^*-\langle U_{AD} \rangle$ relation is used in the wind farm simulation to determine the thrust force for each iteration. The power is calculated from a $C_P^*-\langle U_{AD} \rangle$ relation, as a post processing step, where C_P^* is defined as $C_P^* = (U_H / \langle U_{AD} \rangle)^3$. If one would like to include tangential forces to model wake rotation, it is possible to use a normalized tangential force distribution that is scaled by C_P^* and the tip speed ratio. In the present work, we do not use tangential forces, because its impact on the power deficit is very small (van der Laan et al., 2015b), and it allows us to use the symmetry of the chosen wind farm layout in order to reduce the number of wind directions necessary to calculate the AEP.

The pre-calculated $C_T^*-\langle U_{AD} \rangle$ used in this work is given in Fig. 1, where an additional scaling factor s is added, which is defined as:

$$s = U_H / U_{H,\text{inflow}} \quad (1)$$

where U_H is the freestream wind speed at hub height that one would like to simulate and $U_{H,\text{inflow}}$ is the actual inflow wind speed at hub height in the RANS-AD wind farm simulation. We multiply $\langle U_{AD} \rangle$ in the $C_T^*-\langle U_{AD} \rangle$ by s . This simple scaling allows us to perform one RANS-AD wind farm simulation with a fixed inflow profile (e.g. $U_{H,\text{inflow}} = 10 \text{ m s}^{-1}$), and use the scaling parameter s to simulate different wind speeds U_H (e.g. $U_H = 12 \rightarrow s = 1.2$). The control of the start and stop events of an AD is based on 1D momentum estimate of the freestream velocity, as described in previous work (van der Laan and Abkar, 2019).

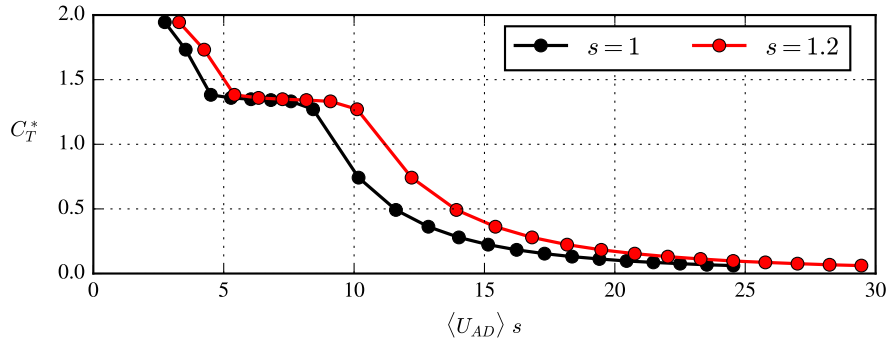


Figure 1. Pre-calculated $C_T^*-\langle U_{AD} \rangle$ curve used for AD control in wind farm simulations. Scaling parameter s is used to represent different wind speeds.

3 Results and Discussion

The AEP of the 5×5 NREL-5MW wind farm is calculated with RANS-AD simulation(s) using 22 wind speeds between 4 and 25 m s^{-1} (every 1 m s^{-1}) and 16 wind directions between $270\text{-}315^\circ$ (every 3°) using the symmetry of the wind farm layout. The wind farm layout is aligned with a wind direction of 270° . A baseline and five additional simulation methodologies are depicted in Fig. 2. The baseline case represents 352 individual simulations, which needs a total of 1.3×10^5 iterations on the

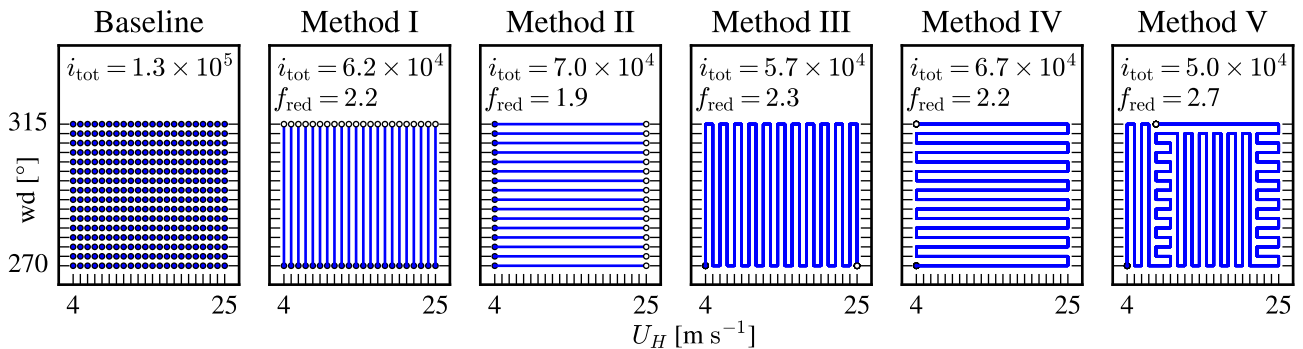


Figure 2. Parallel and sequential simulation methodologies to calculate the AEP using 22 wind speeds (U_H) and 16 wind directions (wd). Filled and open circles represent the start and end flow cases. i_{tot} is the number of iteration on the finest grid level and f_{red} is the reduction of these iterations compared to baseline case.

5

finest grid (i_{tot}). Each simulation is started with a twice as coarse grid (in all three directions) in order to reduce the number of required iterations on the finest grid. The coarse grid CPU time is negligible compared fine grid CPU time and the total number of iterations on the finest grid is representative for the computational effort. Without the multi-grid approach one

would need 2.4 times more iterations for the baseline case (3.2×10^5). The additional methods in Fig. 2 represent sequential or partly sequential simulation(s), where the next wind speed or wind direction is calculated from a previous result. This typically reduces the total number of required iterations because only local flow changes needs to be simulated. However, the required number of iterations is directly proportional to the convergence of the local flow. Therefore, it will not be possible to speed up the computations further by using an initial guess based on *e.g.* one of the fast engineering wake models. The first wind speed and wind direction for Method I-V (filled circles in Fig. 2) is started from a coarser grid level similarly to the Baseline case, while the following wind speed and wind direction are simulated on the finest grid only. The additional methods predict the same AEP within 0.02 % of the Baseline method, which is a result of the chosen convergence criterion. Method I represent 22 separate simulations (one for each wind speed), where the different wind directions are simulated sequentially after each other. The effect of wind direction is simulated by rotating the layout, while keeping the inflow constant. This is possible for RANS-AD simulations using flat terrain and a homogeneous roughness length. The total number of iterations of the finest grid for Method I is reduced by a factor (f_{red}) of 2.2 compared to the Baseline. In Method II, each wind direction is simulated individually and the wind speeds are simulated sequentially using the proposed AD control method from Sect. 2.2, which reduces the number of fine grid iterations by a factor 1.9. Methods III-V are each a single RAND-AD simulation, where all wind speeds and wind directions are simulated by rotation of the layout and scaling of the AD control, respectively. Methods III-V differ in the order of the simulated wind speeds and wind directions. In our presented methods, we choose to either change a wind speed or a wind direction with the smallest step but one could also choose alternative sequential solving paths. This ~~an optimization problems~~ is an optimization problem by itself and it is out of the scope of the present work. Method III and IV provide similar reduction factors, although we have observed that there are differences in the required iterations for particular wind speed and wind direction flow cases. When the thrust coefficient in the wind farm is not varying much (for wind speeds between 7-10 m s⁻¹) and well above rated (> 21 m s⁻¹), it takes less iterations to perform consecutive wind speeds with respect to consecutive wind directions. The opposite is observed for low wind speeds, when some of the wind turbines experience start up and stop events (i.e. when going from 4 to 5 m s⁻¹ or 5 to 4 m s⁻¹) and where the thrust coefficient changes rapidly with wind speed (i.e. above the rated wind speed). Method V is a combination of Methods III and IV in order to further reduce the number of fine grid iteration by a factor 2.7 compared to the Baseline case. It should be noted that performance of Method V is dependent on the thrust coefficient curve and wind farm layout.

For RANS-AD simulations including terrain or in-homogeneous roughness lengths, it is not possible to rotate the layout while keeping the inflow direction constant. In this case, our proposed wind speed independent AD control method would reduce the number of required iteration and computational effort significantly following Method II. Note that RANS simulations of non-homogeneous terrain using a logarithmic inflow and rough wall boundary condition are also independent of the Reynolds number, for wind speeds that are relevant for wind turbines, as discussed by Troen et al. (2014). In addition, if one does not have a multi-grid available to reduce the number of fine grid iterations compared to the Baseline case, then the sequential simulation methods (Methods I-V, which do not benefit much from the multi-grid)) yields an additional reduction factor of 2.4.

The total CPU time of the fastest method (Method V) is 1.4×10^3 CPU hours, representing 4 hours in wall clock time. For non-symmetric wind farm layouts, one would need to perform more wind direction cases, i.e. 120 wind directions, which would increase the CPU hours and wall clock time by a factor of about 7.5 representing a wall clock time of about 30 hours using 352 CPUs. By doubling the amount of CPUs one could achieve an AEP calculation of our test wind farm within a day, which makes the RANS-AD model a feasible tool to validate the AEP of a wind farm designed by engineering wake models. It should be noted that if the user has unlimited computational resources available, then the Baseline method is the fastest in terms of wall clock time compared to Methods I-V because all wind speed and wind direction cases can be performed in parallel, which takes only a few minutes per simulation.

In the present work, we have simulated all wind speeds, also far above rated power where the wind turbines do not experience power losses. If one is only interested in the AEP, then these simulations could have skipped once rated wind farm power is achieved. One could further reduce the computational effort of RANS-AD AEP calculations by reducing the number of wind speed and wind direction cases using statistics of the wind resources (i.e. using the Weibull and wind direction distributions), which could be investigated in future work.

Finally, these computations have been performed with an accuracy of 0.02 % for the convergence error in AEP. One could choose to relax the convergence criteria of the solutions at the expense of an higher error, but with a significant reduction in the total amount of computational iterations. For instance, one could choose to accept an error of 0.5 %, which would reduce the computational effort by a factor of 18. An error of 0.5 % would presumably still be less than the uncertainty associated with for instance the wind rose and C_T -curve of the turbines. The freed computational resources could then be used to examine these larger uncertainties and as the the numerical error has been quantified, one could correct the final AEP assessment accordingly.

4 Conclusions

A simple wind speed independent actuator disk control method is proposed and employed to reduce the number of iterations necessary to calculate the annual energy production from Reynolds-averaged Navier-Stokes simulations of 5×5 rectangular wind farm with a spacing of 5 rotor diameters. The effect of different wind directions and wind speeds are calculated consecutively in a single simulation by rotating the wind farm layout and using the new wind speed independent actuator disk control method, respectively. Since the global inflow wind speed and wind direction are not changed, only local changes need to be re-calculated for every wind speed and wind direction from a previous converged result, which reduces the total number of iterations by a factor of about 2-3. ~~The wind speed independent actuator disk control method has the most potential to reduce the computational effort of annual energy production calculations of wind farm including terrain and in-homogeneous roughness lengths, where the wind farm layout cannot be rotated to calculate the effect of different wind directions.~~

Code and data availability. The numerical results are generated with proprietary software, although the data presented can be made available by contacting the corresponding author.

Author contributions. MPVDL has performed the simulations, produced all figures and drafted the article. SJA and P-ER have contributed to the methodology and finalization of the paper

Competing interests. The authors declare that they have no conflict of interest.

References

- Andersen, S.: Simulation and Prediction of Wakes and Wake Interaction in Wind Farms, Ph.D. thesis, Wind Energy Department, Technical University of Denmark, 2014.
- Barthelmie, R. J., Frandsen, S. T., Nielsen, M. N., Pryor, S. C., Rethore, P. E., and Jørgensen, H. E.: Modelling and measurements of power losses and turbulence intensity in wind turbine wakes at middelgrunden offshore wind farm, *Wind Energy*, 10, 517–528, <https://doi.org/10.1002/we.238>, 2007.
- Göçmen, T., van der Laan, M. P., Réthoré, P. E., Peña Diaz, A., Larsen, G. C., and Ott, S.: Wind turbine wake models developed at the technical university of Denmark: A review, *Renewable and Sustainable Energy Reviews*, 60, 752–769, 2016.
- Jonkman, J., Butterfield, S., Musial, W., and Scott, G.: Definition of a 5-MW Reference Wind Turbine for Offshore System Development, Tech. rep., National Renewable Energy Laboratory, 2009.
- Michelsen, J. A.: Basis3D - a platform for development of multiblock PDE solvers., Tech. Rep. AFM 92-05, Technical University of Denmark, Lyngby, Denmark, 1992.
- Réthoré, P.-E., van der Laan, M. P., Troldborg, N., Zahle, F., and Sørensen, N. N.: Verification and validation of an actuator disc model, *Wind Energy*, 17, 919–937, 2014.
- Richards, P. J. and Hoxey, R. P.: Appropriate boundary conditions for computational wind engineering models using the $k-\epsilon$ turbulence model, *Journal of Wind Engineering and Industrial Aerodynamics*, 46,47, 145–153, 1993.
- Simisioglou, N., Breton, S.-P., and Ivanell, S.: Validation of the actuator disc approach using small-scale model wind turbines, *Wind Energy Science*, 2, 587–601, <https://doi.org/10.5194/wes-2-587-2017>, <https://www.wind-energ-sci.net/2/587/2017/>, 2017.
- Sørensen, N. N.: General purpose flow solver applied to flow over hills, Ph.D. thesis, Risø National Laboratory, Roskilde, Denmark, 1994.
- Sørensen, N. N., Bechmann, A., Johansen, J., Myllerup, L., Botha, P., Vinther, S., and Nielsen, B. S.: Identification of severe wind conditions using a Reynolds Averaged Navier-Stokes solver, *Journal of Physics: Conference series*, 75, 1–13, <http://iopscience.iop.org/article/10.1088/1742-6596/75/1/012053>, 2007.
- Troen, I., Bechmann, A., Kelly, M. C., Sørensen, N. N., Réthoré, P.-E., Cavar, D., and Jørgensen, H. E.: Complex terrain wind resource estimation with the wind-atlas method: Prediction errors using linearized and nonlinear CFD micro-scale models, in: Proceedings of European Wind Energy Association, 2014.
- van der Laan, M. P. and Abkar, M.: Improved energy production of multi-rotor wind farms, *Journal of Physics: Conference Series*, accepted, 2019.
- van der Laan, M. P., Sørensen, N. N., Réthoré, P.-E., Mann, J., Kelly, M. C., and Troldborg, N.: The $k-\epsilon-f_P$ model applied to double wind turbine wakes using different actuator disk force methods, *Wind Energy*, 18, 2223–2240, <https://doi.org/10.1002/we.1816>, 2015a.
- van der Laan, M. P., Sørensen, N. N., Réthoré, P.-E., Mann, J., Kelly, M. C., Troldborg, N., Hansen, K. S., and Murcia, J. P.: The $k-\epsilon-f_P$ model applied to wind farms, *Wind Energy*, 18, 2065–2084, <https://doi.org/10.1002/we.1804>, 2015b.
- van der Laan, M. P., Sørensen, N. N., Réthoré, P.-E., Mann, J., Kelly, M. C., Troldborg, N., Schepers, J. G., and Machefaux, E.: An improved $k-\epsilon$ model applied to a wind turbine wake in atmospheric turbulence, *Wind Energy*, 18, 889–907, <https://doi.org/10.1002/we.1736>, 2015c.

Appendix A: Reynolds number independence of a single wind turbine wake in RANS

The Reynolds number independence of the RANS-AD simulations for a single wind turbine wake is shown in Figure A1, where the stream-wise velocity U , normalized by the inflow wind speed at hub height, $U_{H,\text{inflow}}$, is depicted at a downstream distance of five rotor diameters. The same numerical setup is used as discussed in Section 2, where we use a fixed force distribution scaled by C_T and $U_{H,\text{inflow}}$. We have simulated four different cases representing two thrust coefficients ($C_T = 0.4$ and $C_T = 0.8$) and two ambient turbulence intensities at hub height ($I = 5\%$ and $I = 10\%$) based on the turbulent kinetic energy. Each case is simulated with three different inflow wind speeds, namely, 1, 10 and 100 m s^{-1} , corresponding to a Reynolds number of 8.7×10^6 , 8.7×10^7 and 8.7×10^8 , respectively, for the chosen kinematic molecular viscosity of $1.46 \times 10^{-5} \text{ m}^2 \text{ s}^{-1}$. Figure A1 clearly shows that normalized velocity deficit is independent of the wind speed.

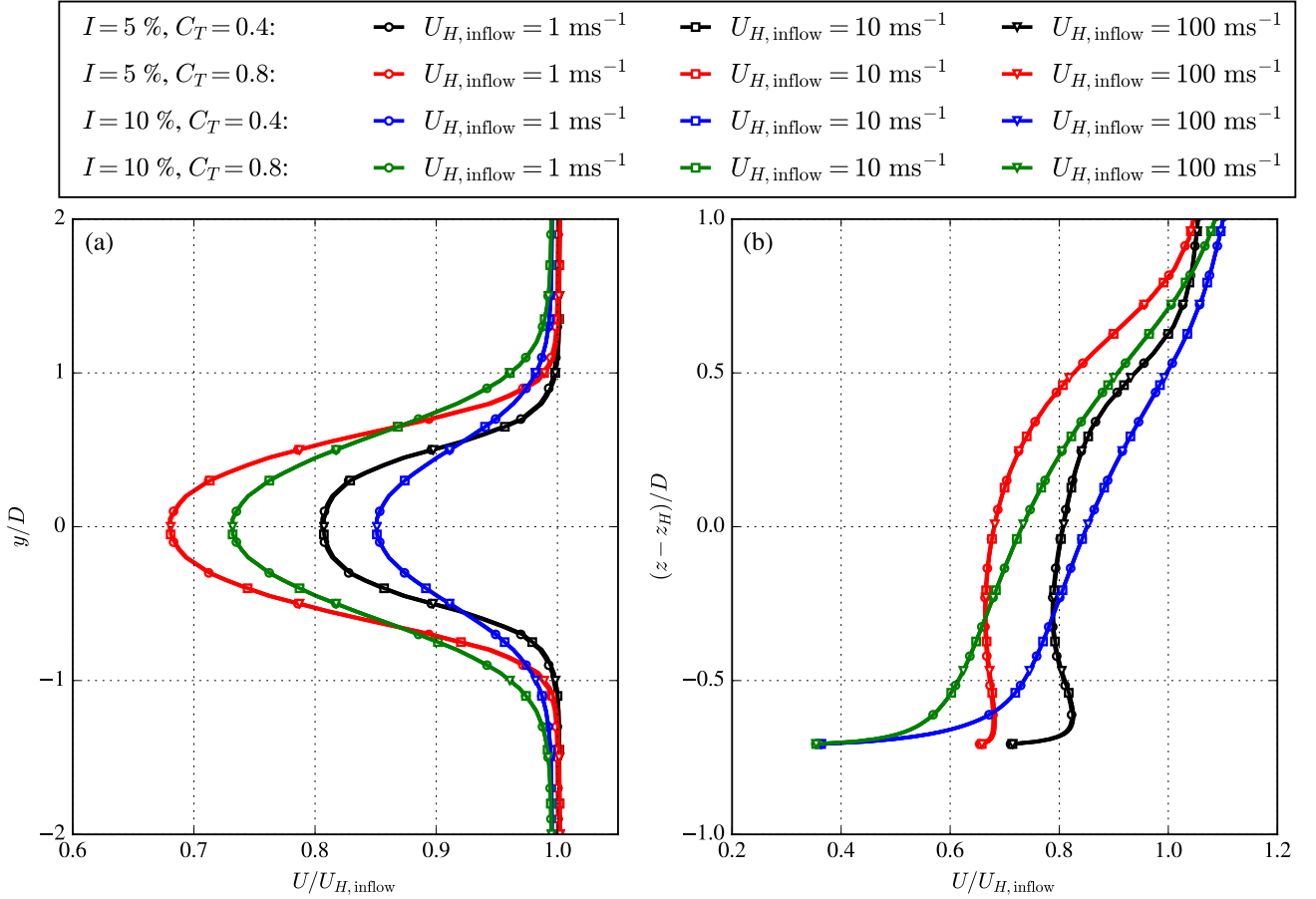


Figure A1. Reynolds number independence of the streamwise velocity deficit of a single AD with a prescribed thrust coefficient C_T and ambient turbulence intensity I , at downstream distance of five rotor diameters. **(a)** Streamwise velocity at hub height as function of the lateral coordinate. **(b)** Streamwise velocity at $y = 0$ as function of the vertical coordinate.